

Accurate Mobility and Energy Relaxation Time Models for SiGe HBTs Numerical Simulation

G. Sasso, N. Rinaldi

Dept. of Electronics and Telecommunications Engineering,
University of Naples "Federico II"
via Claudio 21, 80125 Naples, Italy
grazia.sasso@unina.it

G. Matz, C. Jungemann

Institute for Microelectronics and Circuits,
Bundeswehr University
85577 Neubiberg, Germany

Abstract—Carrier mobility and energy relaxation time analytical models for hydrodynamic simulation of silicon-germanium hetero-junction bipolar transistors (HBTs) have been derived. In addition, some issues related to hydrodynamic simulation in commercial tools are discussed.

Device simulation; SiGe HBTs; Mobility; Energy relaxation time; Hydrodynamic models.

I. INTRODUCTION

Commercial device simulation tools commonly used in industrial applications allow the simulation of Si-based hetero-junction devices, such as SiGe HBTs, with the drift-diffusion (DD) and hydrodynamic (HD) models. However, transport models for DD/HD simulation available in the literature refer to silicon, and do not include the dependence on all relevant parameters (in particular germanium content). This work focuses on the development of calibrated analytical mobility and energy relaxation time models for HD simulation of strained SiGe devices, including the dependence upon the Ge mole fraction. Moreover, some issues related to the HD simulation of SiGe HBTs are discussed.

To generate the transport parameters for HD simulation we use a comprehensive and experimentally verified full-band monte carlo (MC) simulation code [1]. Band structures have been calculated by the non-local empirical pseudo-potential method for biaxial-strained SiGe on relaxed Si for Ge-contents from 0 to 30%.

II. MOBILITY MODEL

Based on MC simulations, an analytical low field mobility model has been developed for both minority and majority carriers. The model formulation is based on an extension to the model of Reggiani *et al.* [2] for silicon, already available in commercial tools. The main model equation (1) allows reproducing accurately the silicon mobility behavior at low and high doping concentration, including dependence upon lattice temperature, T_L , donor and acceptor doping concentration, N_D and N_A , respectively. Here μ_{max} is the lattice mobility, while μ_0 and μ_1 model carrier mobility variations at high and very high doping concentration, respectively. Lattice mobility formulation is modeled by (2), along with μ_0 and μ_1 equations (3) and (4) which allow distinguishing between majority and minority mobility. Moreover, a new formulation for $\mu_{1,d}$ is introduced here [see (5)] in order to extend the model to low

temperatures ($T_L < 300$ K), where some measurements show increasing mobility with doping at very high doping concentration, [3]. The whole set of extracted parameters and equations is reported in TABLE I, where $T_n = T_L/300$ is the normalized lattice temperature. Calibrated silicon model shows a good agreement with experimental data and state-of-art models (Figs. 1 and 2). Majority and minority mobility dependences upon lattice temperature and doping type and values are accurately modeled.

Hetero-junction bipolar transistors simulations need suitable models including the Ge mole fraction dependence. TCADs generally include mobility dependence on mole-fraction applying a linear interpolation between silicon and germanium mobility values or a piecewise polynomial approximation, [10]. However, analytical models are generally preferred for computational reasons and a better physical insight. To the authors' knowledge, the only mobility model including the germanium mole fraction dependence is [11]. This model provides reasonable results only for electrons, while

$$\mu(N_D, N_A, T_L) = \frac{\mu_{\max}(T_L) - \mu_0(N_D, N_A, T_L)}{1 + (N_D/C_{r1}(T_L))^{\alpha_1} + (N_A/C_{r2}(T_L))^{\alpha_2}} + \mu_0(N_D, N_A, T_L) - \frac{\mu_1(N_D, N_A, T_L)}{1 + (N_D/C_{s1}(T_L) + N_A/C_{s2}(T_L))^{-2}} \quad (1)$$

$$\mu_{\max} = \mu_{\max,0} \cdot \left(\frac{T_L}{T_0}\right)^{\gamma} \quad (2)$$

$$\mu_0(N_D, N_A, T_L) = \frac{\mu_{0d} \cdot N_D + \mu_{0a} \cdot N_A}{N_D + N_A} \quad (3)$$

$$\mu_1(N_D, N_A, T_L) = \frac{\mu_{1d} \cdot N_D + \mu_{1a} \cdot N_A}{N_D + N_A} \quad (4)$$

$$\mu_{1,d,a}(N_D, N_A, T_L) = \frac{a(N_D, N_A) \cdot (T_L/T_0)^2 + b(N_D, N_A) \cdot (T_L/T_0) + c(N_D, N_A)}{(T_L/T_0)^2} \quad (5)$$

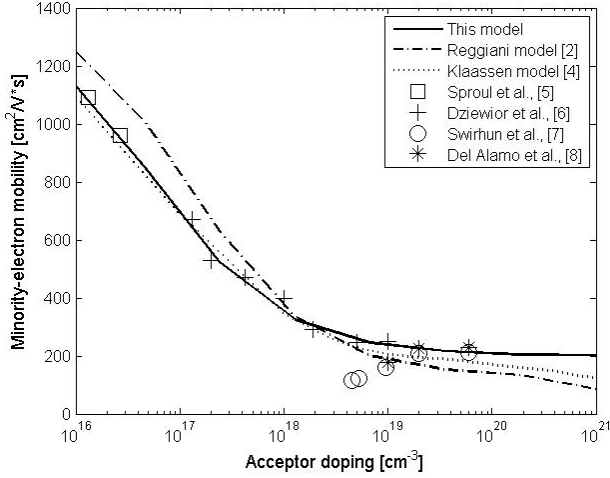


Figure 1. Minority electron mobility in silicon as a function of acceptor doping at 300 K; symbols are experimental data.

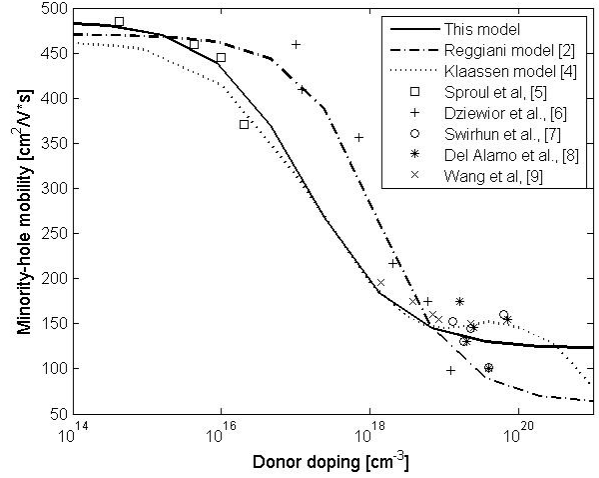


Figure 2. Minority hole mobility in silicon as a function of donor doping at 300 K; symbols are experimental data.

TABLE I. PARAMETERS FOR SILICON BULK MOBILITY

Parameters	Electrons	Holes
$\mu_{\max,0}$ [cm ² /V·s]	1421.6	485.51
γ	-2.24	-2.49
μ_{0d} [cm ² /V·s]	49	$123.34 \cdot T_n^{-1.028}$
μ_{0a} [cm ² /V·s]	$205.25 \cdot T_n^{-0.934}$	$46.42 \cdot T_n^{-0.627}$
μ_{1d} [cm ² /V·s]	$\frac{24.812 \cdot T_n^2 + 84.6 \cdot T_n - 132.36}{T_n^2}$	$\frac{-68.8 \cdot T_n^2 + 300.19 \cdot T_n - 230.53}{T_n^2}$
μ_{1a} [cm ² /V·s]	$\frac{-94.533 \cdot T_n^2 + 518.28 \cdot T_n - 419.15}{T_n^2}$	$\frac{-5.783 \cdot T_n^2 + 81.146 \cdot T_n - 76.02}{T_n^2}$
C_{r1} [cm ⁻³]	$8.393 \cdot 10^{16} \cdot T_n^{2.951}$	$1.329 \cdot 10^{17} \cdot T_n^{3.07}$
C_{r2} [cm ⁻³]	$5.42 \cdot 10^{16} \cdot T_n^{3.045}$	$1.631 \cdot 10^{17} \cdot T_n^{3.111}$
C_{s1} [cm ⁻³]	$1.81 \cdot 10^{19}$	$5.1 \cdot 10^{19}$
C_{s2} [cm ⁻³]	$4.2 \cdot 10^{19}$	$5.8 \cdot 10^{19}$
α_1	0.68	0.7
α_2	0.7	0.77

the Ge content dependence of hole mobility is not well described. Here we propose a new model for SiGe mobility, carefully calibrated for both electrons and holes. The model equation is given by (6), where C_μ is a bowing factor. The germanium content is normalized to 0.3, since in SiGe HBTs the Ge mole fraction never exceeds 0.3 (typically the maximum value is about 0.2). Limiting the mole fraction calibration range improves model accuracy (Figs. 3 and 4).

$$\frac{1}{\mu_{SiGe}} = \frac{1-x_n}{\mu_{Si}} + \frac{x_n}{\mu_{Si_{0.7}Ge_{0.3}}} + \frac{(1-x_n^\alpha) \cdot (x_n^\alpha)}{C_\mu} \quad (6)$$

III. ENERGY RELAXATION TIME MODEL

Macroscopic energy relaxation time is a critical parameter in the HD formulation, appearing in the collision terms of energy balance equation and in high field hydrodynamic mobility model. Accurate verification by MC simulations is needed to achieve consistency of the HD model and the Boltzmann transport equation. A relaxation time model extended to include the mole fraction dependence is given in [13]. This model, however, disregards the dependence on lattice and carrier temperatures. In this work we propose a new analytical model, which incorporates the relaxation time variation with electron and lattice temperature, as well as Ge mole fraction, Figs. 5 and 6. The model equation for energy relaxation times in bulk material is given (7), where the material composition dependence is included through its parameters [see (8) and (9)]. T_n and T_L are the electron and lattice temperature, respectively, and T_0 is the reference temperature of 300 K. Note that, although at low carrier temperature the dependence on carrier temperature changes (Fig. 5), this behavior needs not to be modeled since when the electron temperature is close to the lattice temperature the term $(T_n - T_L)/\tau_w$ appearing in the energy balance equation is negligible.

IV. HBT HYDRODYNAMIC SIMULATION

In the attempt to include non-local effects different formulations for the so called Hydrodynamic or Energy Transport (ET) approximations to the Boltzmann Equation have been proposed [14]. For this reason HD models available in commercial TCAD tools include some tunable parameters which allow switching over different models [10, 15]. The adjustment of equation parameters in HD/ET models has been discussed in a few publications [16]. However, these studies do not mention an unphysical effect which appears in HBT HD/ET simulation with default model parameters, namely a negative slope for output characteristics. In addition, due to the inherent approximations of the HD/ET models, the maximum cut-off frequency can be grossly overestimated.

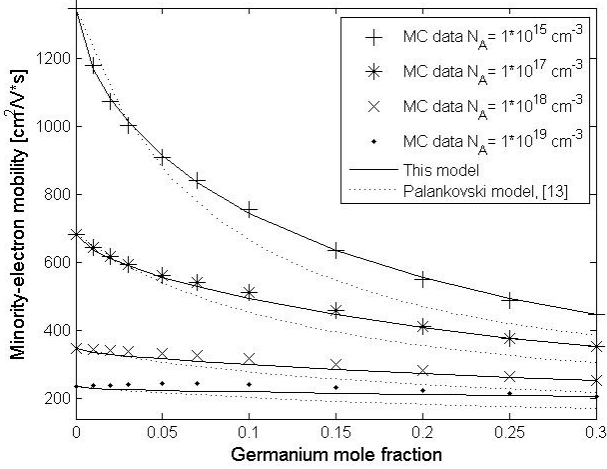


Figure 3. Si_{1-x}Ge_x minority electron mobility as a function of germanium mole fraction (x) for several doping concentrations, T_L = 300 K.

TABLE II. PARAMETERS FOR SiGe ALLOY MOBILITY.

Parameters	Electrons	Holes
α	0.487	0.548
C_{μ} [cm ² /V·s]	2379.4	556.4

TABLE III. PARAMETERS FOR Si_{0.7}Ge_{0.3} BULK MOBILITY.

Parameters	Electrons	Holes
$\mu_{\max,0}$ [cm ² /V·s]	453.23	641.08
γ	-1.14	-2.118
μ_{0d} [cm ² /V·s]	$91.587 \cdot T_n^{-1.0547}$	$130.24 \cdot T_n^{-1.3315}$
μ_{0a} [cm ² /V·s]	$191.58 \cdot T_n^{-0.92012}$	$40.848 \cdot T_n^{-0.63301}$
μ_{1d} [cm ² /V·s]	$\frac{5.494 \cdot T_n^2 + 95.873 \cdot T_n - 96}{T_n^2}$	$\frac{-90.178 \cdot T_n^2 + 325.95 \cdot T_n - 214.83}{T_n^2}$
μ_{1a} [cm ² /V·s]	$\frac{49.072 \cdot T_n^2 + 87.32 \cdot T_n - 131.97}{T_n^2}$	$\frac{3.1834 \cdot T_n^2 + 59.611 \cdot T_n - 57.091}{T_n^2}$
C_{r2} [cm ⁻³]	$1.913 \cdot 10^{17} \cdot T_n^{2.4096}$	$1.3873 \cdot 10^{17} \cdot T_n^{3.2117}$
C_{s1} [cm ⁻³]	$6 \cdot 10^{19}$	$2 \cdot 10^{20}$
C_{s2} [cm ⁻³]	$5.4 \cdot 10^{19}$	$7 \cdot 10^{19}$
α_1	0.76	0.59
α_2	0.7	0.65

$$\tau_w = \tau_{w,0} + \tau_{w,1} \cdot \exp \left(C_1 \cdot \left(\frac{T_n}{T_0} \right)^2 + C_2 \cdot \left(\frac{T_n}{T_0} \right) + C_3 \cdot \left(\frac{T_L}{T_0} \right) \right) \quad (7)$$

$$\tau_{w,0} = \tau_{w,0_{Si}} \cdot (1 - x_n) + \tau_{w,0_{Si_0.7Ge_0.3}} \cdot x_n + C_{\tau} \cdot (1 - x_n) \cdot x_n \quad (8)$$

$$C_1 = C_{1_{Si}} \cdot (1 - x_n) + C_{1_{Si_0.7Ge_0.3}} \cdot x_n + C_C \cdot (1 - x_n) \cdot x_n \quad (9)$$

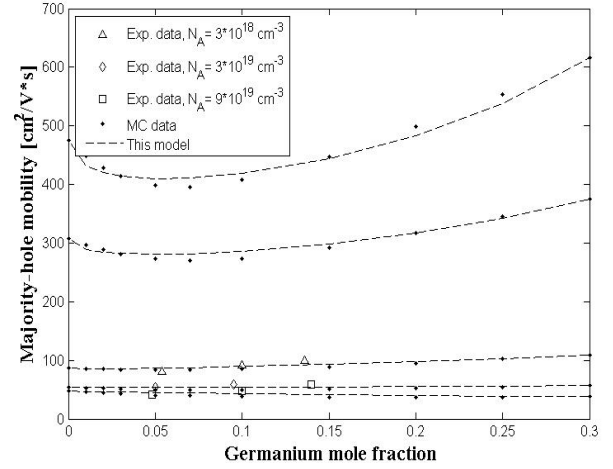


Figure 4. Si_{1-x}Ge_x majority hole mobility as a function of germanium mole fraction (x). Doping values for MC data and model are 10¹⁵, 10¹⁷, 3·10¹⁸, 3·10¹⁹ and 10²¹ cm⁻³ from top to bottom. Experimental data are from [12].

Models equations for the different HD/ET formulations are not reported here for brevity and can be found in [10], where the model parameters are denoted as r , f^{td} and f^{hf} . In the case of the Blotekjaer [17] default model ($r=1$, $f^{td}=f^{hf}=1$) a negative differential resistance in the output characteristics is usually observed. Parameter f^{hf} has a key role in this unphysical effect, since it determines the balance between convective and diffusive components in the energy flux density equation. Since HD models overestimate the heat flux, negative output resistance disappears when f^{hf} is sufficiently small. Simulations of a 100 GHz f_T SiGe test HBT with full-calibrated models have been performed using SDEVICE [10]. Calibrated models also include density of states and high field mobility (not discussed here). The best parameter set for HD simulations was found to be the Blotekjaer model with $f^{hf}=0.2$, providing reasonable results for different structures, yet avoiding negative output resistance. The I_C vs. V_{BE} plot in Fig. 7 shows a good agreement between HD and MC simulations. In addition, we also found that by properly setting equations parameters, the maximum cut-off frequency overestimation, an unavoidable result in HD simulation, is strongly reduced.

TABLE IV. PARAMETERS FOR SiGe ALLOY ENERGY RELAXATION TIME.

Parameters	Electrons
$\tau_{w,0_{Si}}$ [ps]	0.391
$\tau_{w,0_{Si_0.7Ge_0.3}}$ [ps]	0.449
$\tau_{w,1}$ [ps]	-0.14434
C_1_{Si}	0.00135
$C_1_{Si_0.7Ge_0.3}$	0.0028
C_c	-0.00181
C_2	-0.059
C_3	0.0107
C_{τ} [ps]	-0.05

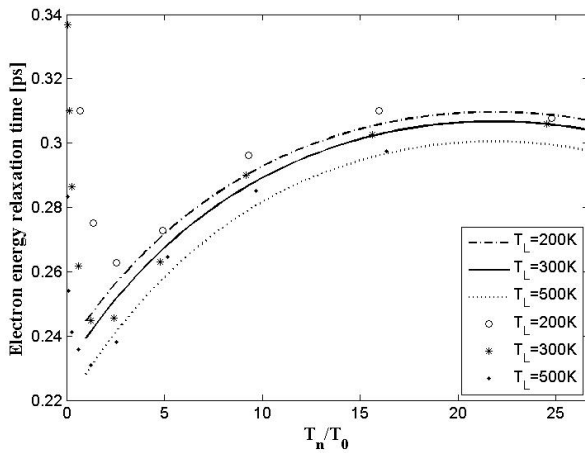


Figure 5. Macroscopic energy relaxation time in silicon as a function of electron temperature for several lattice temperatures, $T_0=300\text{K}$. Lines: model; symbols: MC data.

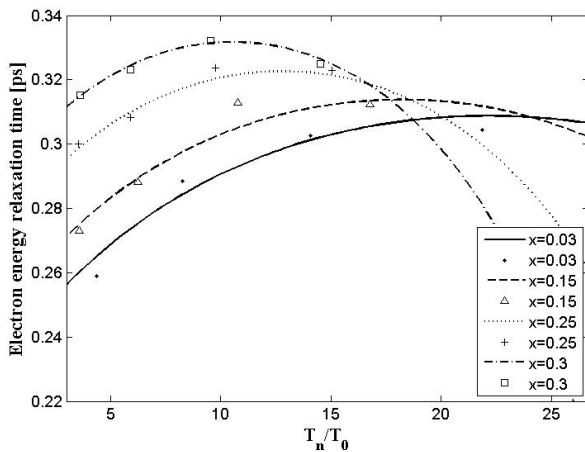


Figure 6. $\text{Si}_{1-x}\text{Ge}_x$ macroscopic energy relaxation time as a function of electron temperature for several germanium contents, $T_L = T_0 = 300\text{K}$. Lines: model; symbols: MC data.

ACKNOWLEDGEMENT

The authors wish to acknowledge the support of the European Commission in the frame of the FP7 IST project DOTFIVE (IST-216110).

REFERENCES

- [1] C. Jungemann, S. Keith, and B. Meinerzhagen, "Full-band Monte Carlo device simulation of a Si/SiGe-HBT with a realistic Ge profile," *IEICE Trans. Electron.*, vol. E83-C, no. 8, pp. 1228-1234, 2000.
- [2] S. Reggiani, M. Valdinocci, L. Colalongo, M. Rudan, G. Baccarani and A.D. Stricker et al., "Electron and Hole Mobility in Silicon at Large Operating Temperatures – Part I: Bulk Mobility," *IEEE Trans. Electron Devices*, vol. ED-49, pp. 490-499, March 2002.

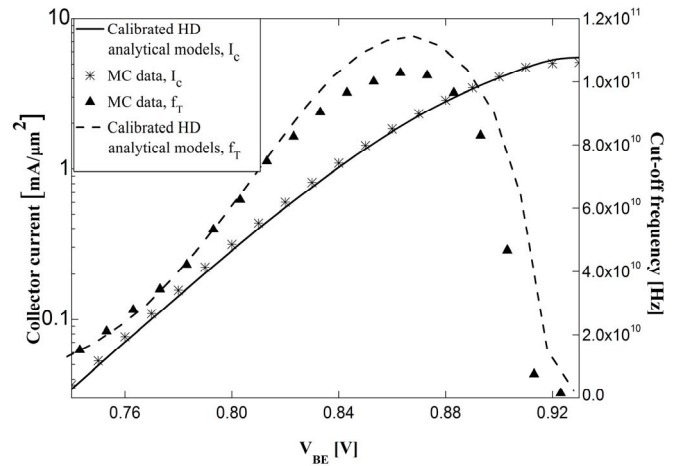


Figure 7. Characteristics of a simulated SiGe HBT: comparison between MC and fully calibrated HD simulations.

- [3] N. D. Arora, J. R. Hauser, and D. J. Roulston, "Electron and Hole Mobilities in Silicon as a Function of Concentration and Temperature," *IEEE Trans. Electron Devices*, vol. ED-29, pp.292-295, Feb. 1982.
- [4] D. B. M. Klassen, "A unified mobility model for device simulation," *IEDM '90*, pp.357-360, September 1990.
- [5] A. B. Sproul, M. A. Green, and A. W. Stephens, "Accurate Determination of Minority Carrier and Lattice Scattering Mobility in Silicon from Photoconductance Decay," *Journal of Applied Physics*, pp. 4161-4171, July 1992.
- [6] J. Dzierwior, and D. Silber, "Minority-Carrier Diffusion Coefficients in Highly Doped Silicon," *Applied Physics Letters*, pp. 170-172, July 1979.
- [7] S. Smirnov, H. Kosina, and S. Selberherr, "Investigation of the electron mobility in strained $\text{Si}_{1-x}\text{Ge}_x$ at high Ge composition," *Proc. Simul. Semicond. Process. Dev.*, pp. 29-32, 2002
- [8] J. A. Del Alamo, S. E. Swirhun, and R. M. Swanson, "Measurement and Modeling of Minority Carrier Transport in Heavily-Doped Silicon," *Solid-State Electron.*, vol. 28, pp. 47-52, 1985
- [9] C.H. Wang, K. Misiakos, and A. Neugroschel, "Temperature Dependence of Minority Hole Mobility in Heavily Doped Silicon," *Applied Physics Letters*, pp. 159-161, July 1990.
- [10] Synopsys TCAD Software, Release 2007.03.
- [11] V. Palankovski, G. Roehrer, T. Grasser, S. Smirnov, H. Kosina, and S. Selberherr, "Rigorous modeling approach to numerical simulation of SiGe HBTs," *Appl. Surf. Sci.*, vol. 224, pp. 361-364, 2004.
- [12] T. K. Carns, S. K. Chun, M. O. Tanner, K. L. Wang, T. I. Kamins, J. T. Turner, D. Y. C. Lie, M.-A. Nicolet, and R. G. Wilson, "Hole mobility measurements in heavily doped $\text{Si}_{1-x}\text{Ge}_x$ strained layers," *IEEE Trans. Electron Devices*, vol. 41, pp.1273-1281, 1994.
- [13] V. Palankovski and R. Quay, *Analysis and Simulation of Heterostructure Devices*. Wien: Springer, 2004.
- [14] T. Grasser, T.-W. Tang, H. Kosina, and S. Selberherr, "A review of hydrodynamic and energy-transport models for semiconductor device simulation," *Proc. IEEE*, vol. 91, no. 2, pp. 251-274, Feb. 2003.
- [15] Atlas Users Manual, SILVACO, 2000.
- [16] I. Bork, C. Jungemann, B. Meinerzhagen, and W. L. Engl, "Influence of heat flux on the accuracy of hydrodynamic models for ultrashort Si MOSFETs," *NUPAD Tech. Dig. Honolulu, HI*, vol. 5, 1994.
- [17] K. Blotekjaer, "Transport equations for electrons in two-valley semiconductors," *IEEE Trans. Electr. Dev.*, vol. ED-17, pp.38-47, Jan. 1970.